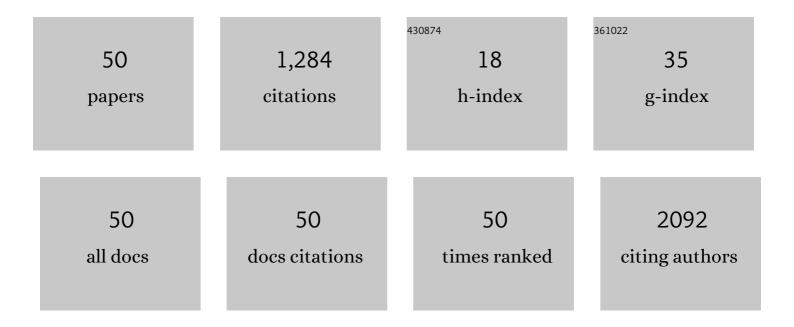
## Maria Pilar Prieto Recio

List of Publications by Year in descending order

Source: https://exaly.com/author-pdf/1906119/publications.pdf Version: 2024-02-01



#	Article	IF	CITATIONS
1	Magnetic domain wall pinning in cobalt ferrite microstructures. Applied Surface Science, 2022, , 154045.	6.1	6
2	Influence of chemical and electronic inhomogeneities of graphene/copper on the growth of oxide thin films: the ZnO/graphene/copper case. Nanotechnology, 2021, 32, 245301.	2.6	1
3	Growth and characterization of ZnO thin films at low temperatures: from room temperature to â"Â120°C. Journal of Alloys and Compounds, 2021, 884, 161056.	5.5	9
4	In-situ study of the carbon gasification reaction of highly oriented pyrolytic graphite promoted by cobalt oxides and the novel nanostructures appeared after reaction. Carbon, 2020, 158, 588-597.	10.3	3
5	Controlled ultra-thin oxidation of graphite promoted by cobalt oxides: Influence of the initial 2D CoO wetting layer. Applied Surface Science, 2020, 509, 145118.	6.1	8
6	Re-Oxidation of ZnO Clusters Grown on HOPG. Coatings, 2020, 10, 401.	2.6	4
7	TiO2 and Co multilayer thin films via DC magnetron sputtering at room temperature: Interface properties. Materials Characterization, 2020, 163, 110293.	4.4	7
8	Tuning the Néel temperature in an antiferromagnet: the case of NixCo1â^'xO microstructures. Scientific Reports, 2019, 9, 13584.	3.3	15
9	Highly oriented (111) CoO and Co3O4 thin films grown by ion beam sputtering. Journal of Alloys and Compounds, 2019, 810, 151912.	5.5	28
10	Epitaxial integration of CoFe2O4 thin films on Si (001) surfaces using TiN buffer layers. Applied Surface Science, 2018, 436, 1067-1074.	6.1	15
11	Geometrically defined spin structures in ultrathin Fe <sub>3</sub> O <sub>4</sub> with bulk like magnetic properties. Nanoscale, 2018, 10, 5566-5573.	5.6	21
12	Structure and magnetism of ultrathin nickel-iron oxides grown on Ru(0001) by high-temperature oxygen-assisted molecular beam epitaxy. Scientific Reports, 2018, 8, 17980.	3.3	27
13	Cross sections of X-ray production induced by C and Si ions with energies up to 1 MeV/u on Ti, Fe, Zn, Nb, Ru and Ta. Nuclear Instruments & Methods in Physics Research B, 2017, 406, 167-172.	1.4	14
14	Fourfold in-plane magnetic anisotropy of magnetite thin films grown on TiN buffered Si(001) by ion-assisted sputtering. Journal of Materials Chemistry C, 2016, 4, 7632-7639.	5.5	7
15	Role of the substrate on the magnetic anisotropy of magnetite thin films grown by ion-assisted deposition. Applied Surface Science, 2015, 359, 742-748.	6.1	11
16	Nanocrystalline magnetite thin films grown by dual ion-beam sputtering. Journal of Alloys and Compounds, 2015, 636, 150-155.	5.5	6
17	Self-organized single crystal mixed magnetite/cobalt ferrite films grown by infrared pulsed-laser deposition. Applied Surface Science, 2015, 359, 480-485.	6.1	11
18	Effects of low energy ion bombardment on the formation of cubic iron mononitride thin films. Thin Solid Films, 2013, 539, 35-40.	1.8	9

#	Article	IF	CITATIONS
19	Photoinduced Pockels effect in the Nd-doped ZnO oriented nanofilms. Applied Physics B: Lasers and Optics, 2013, 110, 419-423.	2.2	27
20	Preparation of hydrosol suspensions of elemental and core–shell nanoparticles by co-deposition with water vapour from the gas-phase in ultra-high vacuum conditions. Journal of Nanoparticle Research, 2012, 14, 1.	1.9	33
21	XPS study of silver, nickel and bimetallic silver–nickel nanoparticles prepared by seed-mediated growth. Applied Surface Science, 2012, 258, 8807-8813.	6.1	456
22	Magnetic antidot arrays on alumina nanoporous membranes: Rutherford backscattering and magnetic characterization. Surface and Interface Analysis, 2011, 43, 1417-1422.	1.8	5
23	Mössbauer spectroscopic study of iron–nickel nitrides thin films prepared by ion beam assisted deposition. Hyperfine Interactions, 2011, 202, 47-55.	0.5	0
24	Structural, Optical and Electrical Properties of ZnO Sprayed Thin Films Doped with Fluorine. Advanced Materials Research, 2011, 324, 253-256.	0.3	3
25	Ordered magnetic nanohole and antidot arrays prepared through replication from anodic alumina templates. Journal of Magnetism and Magnetic Materials, 2008, 320, 1978-1983.	2.3	33
26	Coercive field behavior of permalloy antidot arrays based on self-assembled template fabrication. Journal of Magnetism and Magnetic Materials, 2008, 320, e235-e238.	2.3	27
27	Ferromagnetic resonance and magnetization in permalloy films with nanostructured antidot arrays of variable size. Journal of Magnetism and Magnetic Materials, 2008, 320, e257-e260.	2.3	8
28	Characterization of Nanocrystalline Permalloy Thin Films Obtained by Nitrogen IBAD. IEEE Transactions on Magnetics, 2008, 44, 3913-3916.	2.1	11
29	Structural and magnetic properties of Co <sub><i>x</i></sub> Si <sub>1â^'<i>x</i></sub> thin films and multilayers. Journal of Physics Condensed Matter, 2007, 19, 486003.	1.8	2
30	Hard BCxNy thin films grown by dual ion beam sputtering. Thin Solid Films, 2006, 515, 207-211.	1.8	45
31	Magnetisation dynamics of Fe nanoclusters exchange-coupled to magnetic substrates. Physica Status Solidi A, 2004, 201, 3285-3292.	1.7	0
32	Building high-performance magnetic materials out of gas-phase nanoclusters. Applied Surface Science, 2004, 226, 249-260.	6.1	19
33	Static and dynamic magnetic behaviour of iron nanoclusters on magnetic substrates. Journal of Physics Condensed Matter, 2003, 15, 4287-4299.	1.8	5
34	<title>Control and reduction of post-metal etch corrosion effects due to airborne molecular contamination</title> ., 2001, , .		3
35	Corrective actions for stainless-steel-particle-related burn-in failures. , 2000, , .		2
36	Correlation between bonding structure and mechanical properties of amorphous carbon nitride thin films. Surface and Coatings Technology, 2000, 125, 284-288.	4.8	13

Maria Pilar Prieto Recio

#	Article	IF	CITATIONS
37	Determination of resputtering yields in carbon nitride films grown by dual ion beam sputtering. Surface and Coatings Technology, 2000, 125, 366-370.	4.8	1
38	Dynamics of surface magnetization on a nanosecond time scale. Physical Review B, 2000, 61, R9221-R9224.	3.2	21
39	Magnetic linear dichroism in Gd 4f and 4d photoemission of magnetic interfaces. Journal of Physics Condensed Matter, 1999, 11, 3431-3442.	1.8	0
40	Surface magnetometry with photoemission dichroism:‣Ultrathin epitaxial Fe-Co bcc alloys on Fe(100). Physical Review B, 1999, 59, 4201-4206.	3.2	18
41	Tribological and chemical characterization of ion beam-deposited CNx films. Vacuum, 1999, 52, 199-202.	3.5	13
42	Electronic structure and chemical characterization of ultrathin insulating films. Thin Solid Films, 1998, 332, 209-214.	1.8	16
43	Electronic structure of acetylene onSi(111)â~'7×7:X-ray photoelectron and x-ray absorption spectroscopy. Physical Review B, 1998, 57, 6738-6748.	3.2	46
44	Time-resolved surface magnetometry in the nanosecond scale using synchrotron radiation. Journal of Applied Physics, 1998, 83, 1563-1568.	2.5	21
45	The electronic structure of TiN and VN: X-ray and electron spectra compared to band structure calculations. Solid State Communications, 1997, 102, 291-296.	1.9	38
46	SiCN alloys deposited by electron cyclotron resonance plasma chemical vapor deposition. Applied Physics Letters, 1996, 69, 773-775.	3.3	103
47	Characterization of carbon nitride thin films prepared by dual ion beam sputtering. Applied Physics Letters, 1996, 69, 764-766.	3.3	41
48	Zr-BN multilayers obtained by ion-assisted sputtering: an FT-IR, GAXRD and AES depth profiling characterization. Surface and Coatings Technology, 1996, 84, 392-397.	4.8	1
49	Origin of the surface metallization in single-domain K/Si(100)2×1. Physical Review B, 1996, 54, R14277-R14280.	3.2	10
50	Electronic structure of insulating zirconium nitride. Physical Review B, 1993, 47, 1613-1615.	3.2	61